Bioconjugate Chemistry

Article

pubs.acs.org/bc

Switchavidin: Reversible Biotin–Avidin–Biotin Bridges with High Affinity and Specificity

Barbara Taskinen,[†,‡] Dominik Zauner,[§] Soili I. Lehtonen,[†,∥] Masi Koskinen,[†,‡] Chloe Thomson,[†,‡] Niklas Kähkönen,[†,∥] Sampo Kukkurainen,[†,‡] Juha A. E. Määttä,[†,‡] Teemu O. Ihalainen,[†] Markku S. Kulomaa,[†,∥] Hermann J. Gruber,[§] and Vesa P. Hytönen*[,†,‡]

[†]BioMediTech, University of Tampere, Biokatu 6, FI-33520 Tampere, Finland

[‡]Fimlab Laboratories, Biokatu 4, FI-33520 Tampere, Finland

[§]Institute of Biophysics, Johannes Kepler University, Gruberstrasse 40, 4020 Linz, Austria

[∥]Tampere University Hospital, PL 2000, FI-33521 Tampere, Finland

Supporting Information

ABSTRACT: Switchavidin is a chicken avidin mutant displaying reversible binding to biotin, an improved binding affinity toward conjugated biotin, and low nonspecific binding due to reduced surface charge. These properties make switchavidin an optimal tool in biosensor applications for the reversible immobilization of biotinylated proteins on biotinylated sensor surfaces. Furthermore, switchavidin opens novel possibilities for patterning, purification, and labeling.

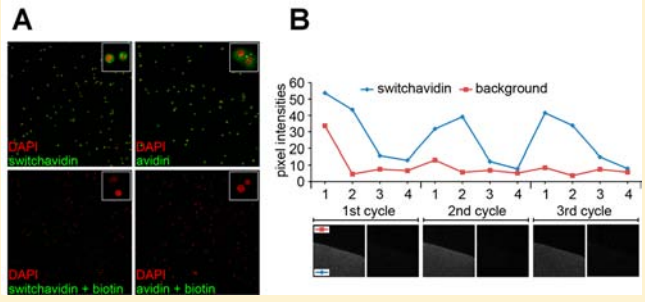

INTRODUCTION

Avidin and streptavidin are homologous tetrameric biotin-binding proteins from chicken and *Streptomyces avidinii*, respectively.[1] The binding to their ligand biotin is practically irreversible, and biotin can be coupled to virtually any target by using chemical coupling or a biotinylation signal, i.e., a peptide tag that is recognized by an ATP-dependent biotin ligase such as BirA.[2] Avidin and streptavidin are therefore used in a broad variety of applications, for example, in affinity purification of biotinylated proteins,[3−5] in targeting and labeling techniques,[6−8] and in immobilization of biotinylated molecules, such as on the surface of a biosensor.[9,10] The tight interaction between (strept)avidin and biotin has an undesired side effect: it is not possible to quickly release the complex between (strept)avidin and a biotinylated substance without harsh treatment. For example, it has been described that release of biotinylated BSA from streptavidin Sepharose can be achieved only by using treatment with 2% SDS, 30 mM biotin, 50 mM phosphate, 100 mM NaCl, 6 M urea, and 2 M thiourea solution (pH 12) for 15 min at room temperature, followed by 15 min at 96 °C, whereas a 30 min incubation in 8 M guadinium hydrochloride, pH 1.3, at room temperature was incapable of releasing the biotinylated BSA.[11] Interestingly, Holmberg et al. described efficient release of terminally biotinylated DNA from streptavidin beads by incubation in salt-free aqueous solution at 70 °C.[12] Similarly, Nguyen et al. demonstrated the release of multibiotinylated molecules from streptavidin in the presence of biotin and high temperatures.[13] However, the release of biotinylated molecules was incomplete.[13] Trials to change the properties of (strept)avidin to enable release of biotin under mild conditions by modifying the biotin-binding pocket resulted in a biotin affinity that was too low,[14] an incomplete modification due to the chemical approach,[15] or a high dissociation rate.[16]

Furthermore, there have been attempts to develop more sophisticated systems for controlled release of (strept)avidin from biotinylated substrates. One example is the attachment of biotin on the target material via oligonucleotides, allowing removal of the bound (strept)avidin layer by dissociation of the hybridized DNA molecules.[17] Another strategy stems from the use of a monolayer of hydrophobic molecules, which enables attachment of biotinylated lipids and their subsequent release by detergents.[18,19] Unfortunately, our recent study revealed that none of these strategies allow complete and robust release of layers consisting of (strept)avidin and (multi)biotinylated proteins.[20] As an alternative, it is possible to utilize chemically cleavable biotinylated linker molecules such as cleavable biotinylated nucleotides[21] or EZ-Link Sulfo-NHS-SS-Biotin (Thermo Scientific) for the immobilization of molecules on a (strept)avidin layer, but this does not allow the substrate to be reused.

We previously reported a switchable avidin mutant, avidin M96H, which was obtained by introducing a histidine residue at the tetramer interface.[22] The additional histidine causes the

Received: October 8, 2014
Revised: November 17, 2014
Published: November 18, 2014

   dx.doi.org/10.1021/bc500462w | *Bioconjugate Chem.* 2014, 25, 2233−2243

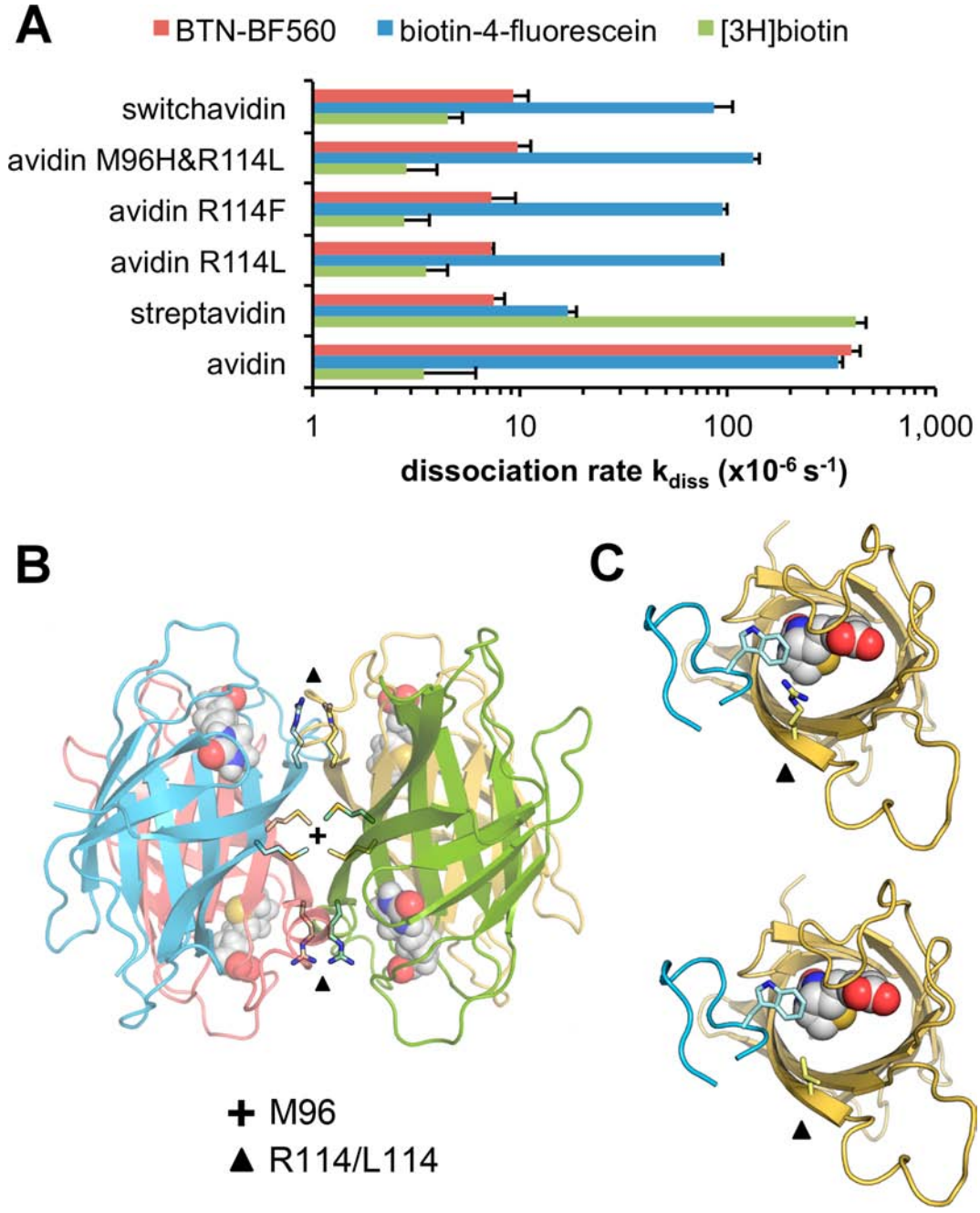

Figure 1. Mutation R114L enhances binding of conjugated biotins. (A) Dissociation rate constants (k_{diss}) of biotin probes from avidin mutants at 50 °C (see also Table S1 and Figure S1). Error bars display the standard deviation calculated from three measurements. (B) Location of M96H and R114L in the tetrameric structure of avidin and (C) close-up view of the biotin-binding site of avidin (top) and avidin R114L (bottom).

avidin tetramer to disassemble into its monomers by the combination of mild acid with SDS.[20] This allowed us to prepare regenerable biosensor chips by repeated formation and destruction of biotin−avidin−biotin bridges on the biotinylated sensor's surface by the complete removal of avidin from the biotinylated surface.[20] Unfortunately, avidin M96H showed high nonspecific binding, due to its positive surface charge at neutral pH. The adsorption problem was reduced by acetylation of avidin M96H, but adverse side effects resulted from the statistical nature of acetylation.[20] Another drawback of avidin M96H is that avidin has been found to bind conjugated biotins with lower affinity as compared to that of streptavidin.[23]

Here, we describe an improved variant of avidin M96H that addresses these challenges. Mutation M96H is combined with mutations tailoring the surface of the protein, resulting in low nonspecific binding. By mutating residue 114, close to the opening of the ligand-binding site, we were able to improve the binding affinity toward conjugated biotin. The resulting protein, switchavidin, can be attached on biotinylated substrates to create an avidinylated surface, which, in turn, can be further functionalized with other molecules via attached biotins. After the desired function, the system can be reversed to its original state by completely removing the avidin layer form the biotinylated substrate with a mild treatment.

dx.doi.org/10.1021/bc500462w | *Bioconjugate Chem.* 2014, 25, 2233−2243

RESULTS AND DISCUSSION

Mutation R114L Increases the Affinity of Avidin and Avidin M96H toward Conjugated Biotin. In avidin–biotin technology, biotin is typically conjugated to a target material/molecule. However, avidin's affinity toward biotin is drastically decreased when biotin is conjugated to other molecules (Figure 1A, red and blue bars). The dissociation rate of free biotin from streptavidin is ∼100-fold higher as compared to that from avidin (Figure 1A, green bars), and the dissociation rate of conjugated biotin from streptavidin is ∼100-fold lower as compared to that from avidin (Figure 1A, red and blue bars), in accordance with earlier findings.[23] In order to improve the binding of avidin to conjugated biotin, we selected arginine 114 as a target for mutagenesis because we found that it formed transient interactions with dissociating biotin in steered molecular dynamics simulations (not shown). A previous structural analysis also identified interactions between R114 and biotin-conjugated molecules[24] (Figure 1B). Bulky amino acids leucine and phenylalanine were selected, based on molecular modeling and on the comparison with related proteins (streptavidin has a leucine in this position). We first studied the effects of the mutations on the thermal stability of avidin by using differential scanning calorimetry. The introduction of the mutation R114L to avidin had only a minor effect on the thermal stability, whereas in the case of avidin R114F, the thermal transition midpoint (T_m) was decreased by 19.3 °C as compared to that of the wild-type protein (Table 1). To evaluate the binding of biotin, the dissociation rate constant (k_{diss}) of tritiated biotin was determined and found to be closely similar to that of the wild-type protein in both mutants (Figure 1A and Table S1). In conclusion, R114 does not appear to be important for the binding of unconjugated biotin. However, the dissociation rates of conjugated biotins (fluorescently labeled biotin BF560–biotin and biotin–4-fluorescein) decreased by more than 40-fold for both avidin R114L and avidin R114F in comparison to that of WT avidin, which places it in the range of the dissociation rate of conjugated biotins from streptavidin (Figure 1A and Table S1). In addition, the association rate constant of conjugated biotin was increased by more than 1.5-fold in avidin R114L and 2-fold in avidin R114F (Figure S1).

Table 1. Thermal Stability (Thermal Transition Midpoint, T_m) Determined by Differential Scanning Calorimetry[a]

protein	(−) biotin	(+) biotin	ΔT_m (biotin)
WT avidin	78.1 ± 0.4	119.6 ± 1.1	41.5
streptavidin	78.5 ± 0.6	112.0 ± 0.1	33.5
avidin R114L	74.7 ± 0.3	117.9 ± 1.1	43.2
avidin R114F	58.7 ± 0.7	115.3 ± 0.6	56.6
avidin M96H	56.2 ± 0.2	117.5 ± 0.2	61.3
avidin M96H/R114L	53.6 ± 0.2	114.9 ± 0.1	61.3
switchavidin	52.0 ± 0.3	114.2 ± 0.1	62.2

[a]Average T_m values and errors are calculated from three measurements.

Therefore, by comparing the association rate constants (Figure S1) and dissociation rate constants (Table S1) determined for WT and mutated avidins, we found 90- and 115-fold increases in the binding affinity of conjugated biotin at 50 °C resulting from mutations R114L and R114F, respectively. This comparison assumes similar differences between proteins in the association kinetics over the temperature range from 25 to 50 °C, which is justified by the close structural similarity of the mutants. Overall, the introduction of mutation R114L is more beneficial than that of mutation R114F, due to the negative effect of R114F on the thermal stability. We therefore chose mutation R114L for further use.

It is tempting to compare our results with other studies aimed at increased affinity toward biotin or biotinylated molecules: Despite numerous studies in the field, only a small number of studies have reported increased binding affinities for avidin proteins. Recently, Chivers et al. described traptavidin,[25] a streptavidin form carrying mutations S52G and R53D in the loop connecting β-strands 3 and 4, which can be considered as a lid shielding the bound ligand from the surrounding solvent. They observed >10-fold decrease in the biotin dissociation rate as compared to that for WT streptavidin as well as a ∼10-fold decreased association rate, thus resulting in a roughly 2-fold higher affinity for free biotin. They also reported a decreased association rate (2-fold decrease) and dissociation rate (not quantified) for biotin–4-fluorescein. Another study utilized a *in vitro* compartmentalization method to select streptavidin variants with tight binding to desthiobiotin.[26] One of the resulting protein variants, R7-6, showed a ∼50-fold decrease in the dissociation rate of the desthiobiotinylated DNA complex, but it also had a ∼50-fold decreased association rate, thus resulting in an insignificant change in binding affinity. Our avidin R114L differs from traptavidin and R7-6 by having a simultaneous decrease in the dissociation rate and increase in the association rate of conjugated biotin.

Next, we applied mutation M96H to avidin R114L to introduce the regeneration capability. Mutation M96H caused a decrease in thermal stability by 25.7 °C (Table 1). Nevertheless, the protein avidin M96H/R114L was found to be tetrameric (Figure S2), and mutation M96H did not compromise the tight binding of conjugated biotin (Figure 1A). Therefore, we were able to improve the biotin-binding characteristics of avidin M96H with the introduction of mutation R114L.

However, it is not simple to explain how mutation M96H causes a drop in thermal stability without affecting the biotin-binding affinity: First, it is important to keep in mind that the relation between ligand-binding affinity and thermal stabilization has several parameters, and ΔT_m alone cannot be used as a measure of ligand-binding affinity.[27] Second, in the case of avidin and other oligomeric proteins, high thermal stability in the presence of the ligand may reflect both increased stability of the protein subunit and increased stability of the tetrameric assembly, as described earlier by González et al.[28] In the case of M96H avidin, tetrameric assembly of the protein can be destroyed by exposing the protein to low pH, as shown by size-exclusion chromatography.[22] However, only tetrameric species are present when the same analysis is performed in the presence of the ligand.[22] We thus observe that biotin binding controls the penetration of water and ions to the subunit interface. Importantly, this is not limited to avidin mutant M96H. An extensive study by Katz[29] revealed that the configuration of subunit–subunit interactions at low pH was affected by the presence of biotin in streptavidin. Therefore, we propose that the ligand-binding affinity and the stability of the (strept)avidin tetramer are tightly interlinked. Although there may not be clear cooperativity between the binding sites,[28,30] the presence of tetrameric structure is a prerequisite for tight

dx.doi.org/10.1021/bc500462w | Bioconjugate Chem. 2014, 25, 2233–2243

ligand binding.[31] In the case where the tetrameric assembly is compromised by mutations, ligand binding may have a more dramatic effect on the thermal stability, as shown here for M96H-containing avidin forms. In other words, M96H mutation increases the importance of biotin binding in the structural cooperativity between the subunits.

We can find further support for this model from the results observed earlier for avidin interface mutant I117Y.[32] This mutation is located in the same subunit interface as that of M96H, but it has a stabilizing effect, leading to an increased T_m of 14 °C in the absence of ligand. However, the stability in the presence of ligand exceeded the T_m of WT avidin by only 6.7 °C, leading to a smaller ΔT_m than that measured for WT avidin. However, avidin I117Y had a decreased biotin dissociation rate as compared to that of WT avidin. Therefore, it appears that the dynamics of the (strept)avidin tetramer is tightly involved in the ligand dissociation process. Indeed, it has been previously proposed that water movement within the interface between the subunits of the tetramer is a key factor regulating the dissociation of biotin from streptavidin.[33] Not surprisingly, disruption of the tetrameric assembly of (strept)-avidin leads to a radically decreased biotin-binding affinity, as was demonstrated by several studies.[14,34−36] Taking into account the importance of water movement and structural dynamics of the protein for the tight ligand binding, it might be impossible to reach affinities comparable to that of chicken avidin or streptavidin without oligomeric structure.

Mutations K9E, R124H, and K127E Lower the Net Charge of Avidin M96H without Affecting Its Physicochemical Properties. Our preceding study showed that undesired nonspecific binding of protein to avidin M96H was successfully suppressed by chemical acetylation. At the same time, the statistical nature of acetylation produced a significant fraction of overacetylated proteins with reduced stability.[20] Now, we genetically engineered avidin M96H by introducing neutralizing mutations to improve the stability of the protein (we found chemically acetylated M96H to suffer from long-term storage at −25 °C) and to ensure full homogeneity of protein preparations. We first tested the neutralizing mutations described in an earlier study,[37] but the resulting avidin would not express in *Escherichia coli*, and it showed poor yield when produced in insect cells. Therefore, we carefully consulted the previously determined X-ray structures of avidin (2AVI), AVR2 (1WBI), and AVR4 (1Y55)[31,38,39] and selected residues that have no important role in the structural integrity of the tetramer or in ligand binding. On the basis of this information, we constructed switchavidin by introducing the three neutralizing mutations, K9E, R124H, and K127E, in avidin M96H/R114L, which resulted in an experimental isoelectric point of ∼7 (Figure S3), close to that estimated based on the polypeptide sequence (7.1). The resulting mutant protein, named switchavidin, was robustly expressed in *E. coli*, and the neutralizing mutations had no effect on thermal stability (Table 1), biotin-binding characteristics (Figure 1A and Table S1), or oligomeric structure (Figure S2).

Switchavidin Forms Highly Specific Biotin−Avidin−Biotin Bridges. Switchavidin was well-suited to form reversible biotin−avidin−biotin bridges on a biotinylated biosensor's surface, as previously shown for avidin M96H on a biotinylated self-assembled monolayer (SAM, with biotin on 20% of the SAM components[20]) and the subsequent binding of biotin−IgG on the switchavidin surface. The switchavidin−biotin−IgG layer was completely removed by treatment of the surface with 2.5% citric acid and 0.25% SDS, followed by 0.5% SDS. The same cycle was performed in triplicate with avidin M96H, avidin M96H/R114L, and switchavidin (Figure 2B). The average layer thickness of the three avidin mutants measured in flow cell 1 (FC1) was 2507 ± 15 RU, 2494 ± 3 RU, and 2416 ± 8 RU, respectively. These values were used as reference values (100%). The other resonance angles measured with the same mutant were normalized to these reference values. The baseline drift between the start and end of each cycle (Figure 2A) was also normalized to the reference value. As can be seen from the bar diagram in Figure 2B, the baseline drifts were usually negligible (<1.2% of the avidin layer thickness in FC1). The slightly higher drift (2.2 ± 2.2%) measured with avidin M96H was due to the fact that these experiments were performed on a new chip that had not been used before. The reproducibility of mutant layer thickness values was very good, as can be seen from the low standard deviation values measured with all mutants in FC1 (Figure 2B, red bars without fill) and flow cell 2 (FC2; Figure 2B, blue bars without fill). The reproducibility of the biotin−IgG layer on top of avidin is also very good (Figure 2B, green bars with yellow fill); only with switchavidin was the standard deviation slightly higher (±2.7%). These data confirm that the switchavidin-functionalized biosensor surface is reliably regenerated multiple times with very low deviation in the thickness of the layers of bound molecules between cycles.

The observed layer thickness is similar to that measured earlier for streptavidin (∼3000 RU).[20] The slightly lower thickness observed for the avidin variants might reflect a less regular arrangement on the surface as compared to that with streptavidin, which is known to form highly ordered 2D crystals on lipid monolayers containing biotinylated lipids.[40] A previous study has shown that the binding signal in SPR measurements can be converted to layer thickness so that 1000 RU corresponds to 1 ± 0.1 ng/mm^2.[41] On the basis of this model, 2500 RU corresponds to a lateral density of 2.5 ng/mm^2 (or 2.5 mg/m^2). Assuming a protein density of 1.35 g/cm^3, 2.5 mg/m^2 corresponds to a layer thickness of 1.85 nm effective height. This clearly suggests that we have a loosely packed monolayer of avidin, as expected for a random distribution of fixed biotins on the SAM surface (shown for sulfonamide ligand and carboanhydrase binding by Lahiri et al.).[42]

To determine the extent of nonspecific binding of analyte molecules to switchavidin, the specific binding (hybridization) and nonspecific adsorption of DNA on monolayers of switchavidin was compared with the performance of avidin M96H and avidin M96H/R114L (Figure 3). In the experiment shown in Figure 3A, FC2 was functionalized with switchavidin, followed by binding of biotinylated single-stranded DNA (biotin probe). Subsequently, the control cell (FC1) was also functionalized with switchavidin, and both cells were treated with BSA to minimize nonspecific adsorption. Next, the complete absence of nonspecific adsorption of DNA on switchavidin was demonstrated by injection of unlabeled DNA, which had the identical sequence as that of the biotin probe; no increase in the resonance angle was seen in FC1 and FC2.

Finally, the complementary DNA strand (analyte DNA) was injected into both flow cells, resulting in pronounced hybridization to the immobile biotin probe in FC2 and complete absence of nonspecific adsorption in FC1 where no biotin-probe had been immobilized. The experiment shown in Figure 3A was performed with the three avidin mutants avidin

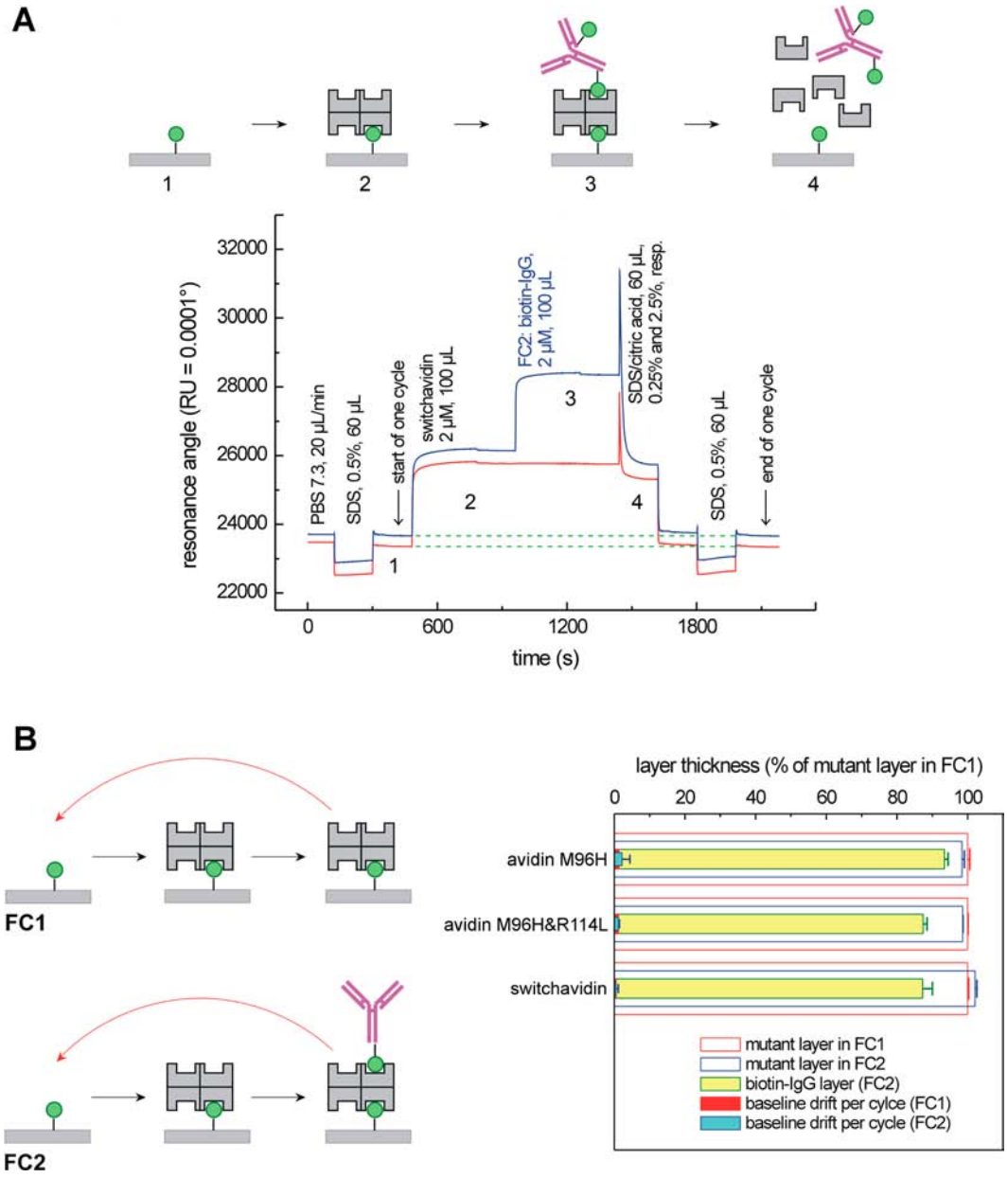

Figure 2. Reversible binding of switchavidin (±biotin−IgG) on a biotinylated self-assembled monolayer (SAM). (A) Outline of the experiment. After the measurement cycle, the proteins were completely removed by regeneration buffer (2.5% citric acid and 0.25% SDS) and SDS (0.5%). The binding and release of switchavidin and biotin−IgG are schematically shown above the sensorgram. Numbers in the scheme refer to the corresponding steps in the sensorgram. (B) High reproducibility of reversible binding of avidin M96H, avidin M96H/R114L and switchavidin to biotin−IgG on a biotinylated SAM.[20] FC1 was functionalized with mutant avidin only, whereas FC2 was additionally functionalized with biotin−IgG, as shown in the schematic representation.

M96H, avidin M96H/R114L, and switchavidin. Magnified traces from the analyte DNA injection (late period of Figure 3A) are shown in panels B and C of Figure 3. Flow cell 1 contained no biotin probe; therefore, the corresponding traces in Figure 3C reflect only nonspecific adsorption of DNA to the avidin mutants. The extent was high on avidin M96H (blue trace), intermediate on avidin M96H/R114L (red trace), and negligible on switchavidin, where only a slight bulk effect was seen (green trace). Flow cell 1 contained the biotin probe; thus, the corresponding traces in Figure 3B were expected to reflect both hybridization and nonspecific adsorption. The comparison of Figure 3, panels B and C, indicates, however, that only hybridization is seen on switchavidin (green trace in Figure 3B), whereas the larger signals for the other avidin mutants are caused by adsorption that occurs in addition to hybridization (blue and red traces in Figure 3B).

Switchavidin also exhibited reduced nonspecific binding toward protein analyte molecules (Figure 4). Panel A shows the standard test experiment on switchavidin. It was performed in triplicate with all three avidin mutants (see Table S2), and representative results are depicted in Figure 4B. Nonspecific binding of BSA (filled bars) was strongly reduced in the series: avidin M96H > avidin M96H/R114L > switchavidin. The tendency was less pronounced for IgG binding (red bars without fill), due to the beneficial effect of BSA pretreatment. The latter findings conform to our previous findings that avidin

dx.doi.org/10.1021/bc500462w | Bioconjugate Chem. 2014, 25, 2233−2243

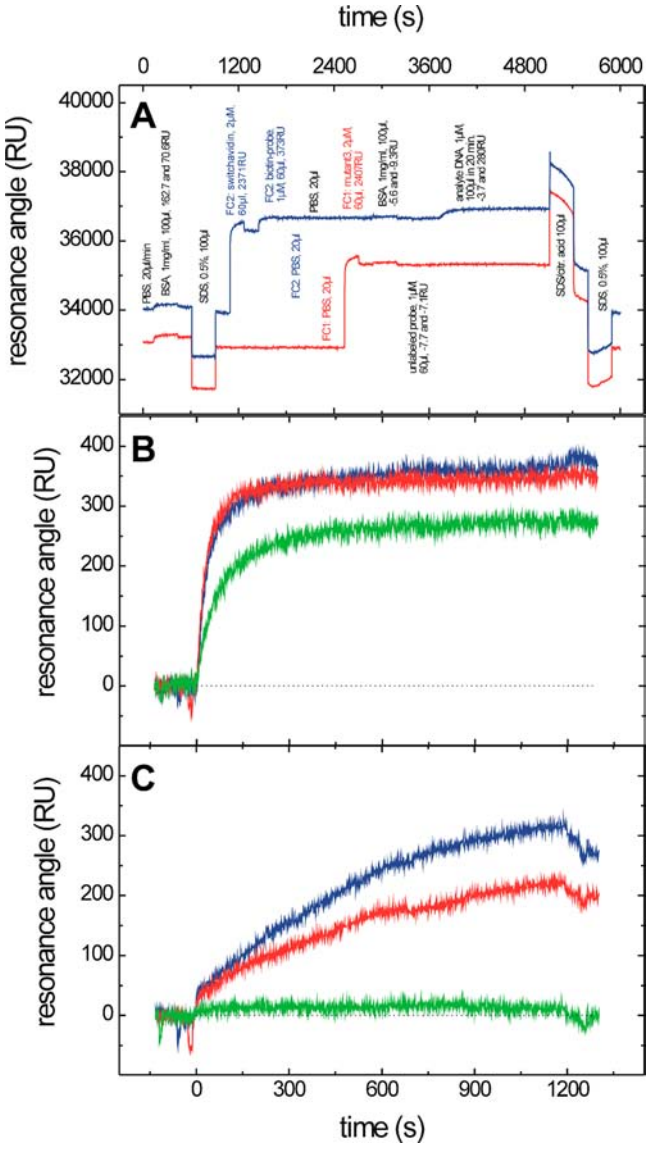

Figure 3. Characterization of specific binding (hybridization) and nonspecific adsorption of DNA on monolayers of the different avidin mutants. (A) Measurement of hybridization between biotinylated single-stranded DNA (immobilized on switchavidin) and the complementary oligonucleotide. Specific binding was probed in FC2, whereas nonspecific binding was probed in FC1. Labels in black refer to reagents added to both flow cells, whereas labels in red and blue refer to reagents added to FC1 or FC2 only, respectively. The experiment is exemplified for switchavidin, but it was also performed with avidin M96H and with avidin M96H/R114L in separate runs (not shown). (B) Expanded view of the response to the analyte DNA in FC2, corresponding to the sum of specific binding (hybridization) and nonspecific adsorption on switchavidin (green), avidin M96H (blue), and avidin M96H/R114L (red). (C) Switchavidin (green) shows a low amount of nonspecific binding. Expanded view of the response to the analyte DNA in FC1, corresponding to nonspecific adsorption only. The color code is the same as that in panel B.

with M96H mutation alone can well be used for protein interaction studies, provided that nonspecific binding of protein is suppressed by binding of biotin–BSA and BSA.[20] Nevertheless, Figure 4 shows that switchavidin offers further improvement over avidin M96H when studying protein interaction. It can be summarized that switchavidin seems generally to be the optimal choice for reversible biofunctionalization of sensor surfaces, being indispensable for nucleic acid analytes (Figure 3) and beneficial for protein analytes (Figure 4).

Switchavidin Is Suitable for Reversible Labeling of Biotinylated Cells and Surfaces. Besides biosensor applications, fluorescently labeled switchavidin was found to be suitable for labeling of biotinylated mammalian cells (Figure 5A), and the specificity of the labeling was confirmed by blocking the interaction with free biotin (Figure 5A). The suitability of switchavidin for reversible labeling of biotinylated patterns on glass was demonstrated by covalently coupling biotinylated BSA on aminosilanized glass and by visualizing the pattern with fluorescently labeled switchavidin (Figure 5B). The bound switchavidin was then washed away with low pH/SDS treatment, followed by subsequent labeling rounds.

In conclusion, switchavidin enables preparation of avidinylated materials in a regenerable manner, displaying high affinity and specificity. Switchavidin thus makes it possible to reuse biotinylated surfaces (sensors, patterns, particles, chromatography gels, etc.) multiple times for immobilization and controlled release of biotinylated molecules or particles, with the number of regeneration cycles being limited only by the chemical stability of the underlying surface itself. However, the technology demonstrated here makes it necessary to attach a new avidin layer on the biotinylated material after each cycle. This may limit the applicability of the technology for tasks such as purification of biotinylated materials. For biosensing and bioanalytical assays, however, this design offers significant advantages over the irreversible immobilization of (strept)-avidin with switchable biotin-binding sites: (i) biotinylated substrates are easily prepared and commercially available for many applications and (ii) perfect switching from completely stable biotin–avidin–biotin bridges under measurement conditions to complete removal of the biotinylated molecules during regeneration has not yet been demonstrated for (strept)avidins with engineered biotin-binding sites. Furthermore, despite the vast amount of avidin–biotin technology tools available, the combination of reversibility with high affinity and specificity is unique, and the availability of switchavidin opens possibilities for completely new approaches.

EXPERIMENTAL PROCEDURES

Cloning of Avidin Mutants. OmpA WT avidin pET101/D[43] was used as the template from which all other mutants were constructed. Mutations M96H, R114L, and R114F were constructed by introducing the respective mutation to OmpA WT avidin pET101/D by QuikChange mutagenesis according to the manufacturer's instructions (Stratagene, La Jolla, CA, USA). OmpA avidin M96H/R114L was subsequently constructed by a second QuikChange mutagenesis using OmpA avidin M96H as the template. Primer sequences are listed in the Supporting Information.

Neutralizing mutations K9E, R124H, and K127E were introduced in a two-step PCR procedure by sequence overlap extension.[44] The 5′ end was amplified using primers Chim_to_2_5′ and K9E_3′. The 3′ end was amplified using primers for_AVD_5′ and R124H_K127E_3′. The two ends were combined in a PCR reaction using primers Chim_-to_2_5′ and R124H_K127E_3′. PCR intermediates and full-length products were analyzed on a 1% agarose gel (Top Vision LE GQ Agarose, Fermentas) and purified from the gel with Illustra GFX PCR DNA and Gel Band Purification Kit (GE Healthcare, Buckinghamshire, UK). The purified full-length

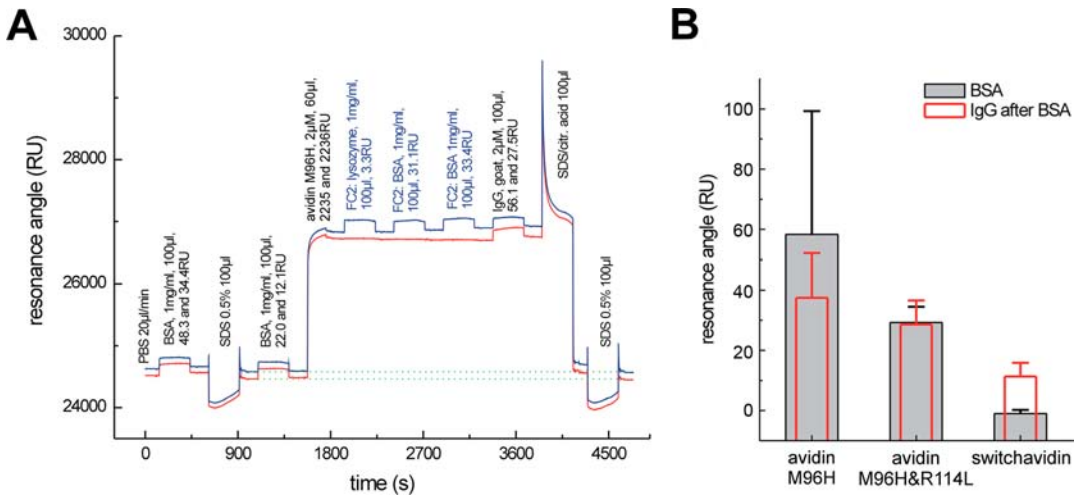

Figure 4. Specific and nonspecific binding of protein analytes on monolayers of the avidin mutants. (A) Analysis of nonspecific binding of representative proteins (hen egg lysozyme, BSA, goat IgG) to a monolayer of avidin M96H that had been immobilized on a biotinylated SAM. The same experiment was performed in triplicate on each avidin mutant. The results for the observed extent of protein adsorption are reported in Table S2 (average ± SD). (B) Nonspecific binding of BSA and goat IgG on monolayers of avidin M96H, avidin M96H/R114L, or switchavidin. Standard deviations are indicated by unilateral error bars to avoid data overlap.

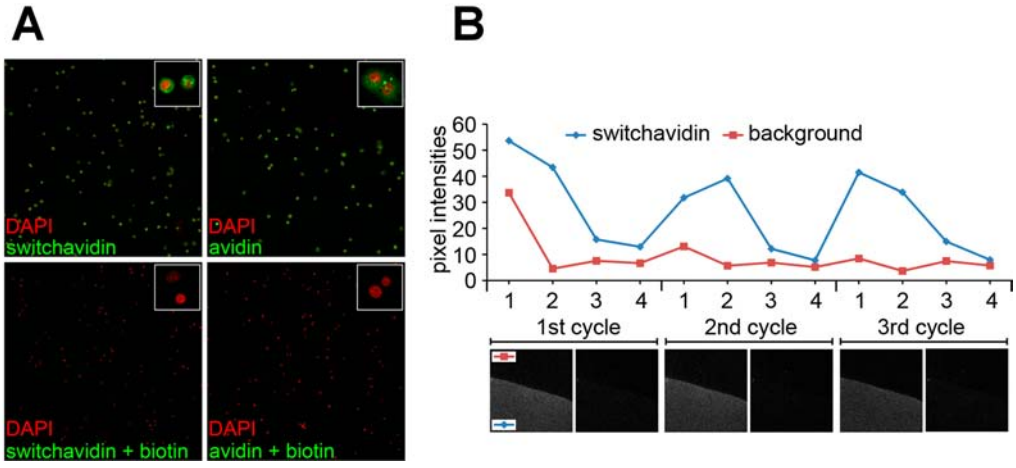

Figure 5. Switchavidin as a regenerable surface labeling agent. (A) Cells stained with fluorescently labeled switchavidin and avidin. Control experiment (lower panels) indicates high specificity of the labeling. (B) Reversible binding of fluorescently labeled switchavidin to biotinylated BSA on a glass surface: (1) fluorescently labeled switchavidin added, (2) excess switchavidin removed with PBS + 1 M NaCl wash, (3) regeneration with 2.5% citric acid + 0.5% SDS, and (4) wash with PBS + 1 M NaCl. The intensity of the regions indicated in the captured snapshots was determined by averaging the intensity over an area of 500 μm^2. Three out of five performed cycles are shown.

PCR products were cloned into the pET101/D plasmid (Invitrogen, Carlsbad, CA, USA) using the TOPO cloning protocol followed by a standard heat shock transformation of chemically competent Top10 *E. coli* cells (Invitrogen). The cells were grown overnight at 37 °C after plating them onto an LB (Lysogeny Broth) medium plate containing ampicillin (100 μg/mL). Ampicillin-resistant colonies were used to isolate the plasmid with GeneJET Plasmid Miniprep Kit (Fermentas International Inc., Thermo Fisher Scientific Inc., Waltham, MA, USA). The sequences of the constructs were confirmed using the BigDye Terminator v3.1 Cycle Sequencing Kit (Applied Biosystems, Carlsbad, CA, USA).

Protein Production of Neutralized Avidin Mutants. The pET101/D vector containing the mutated avidin gene was transformed into *E. coli* BL21-AI (Invitrogen) cells. Single colonies were grown overnight in 10 mL of LB medium containing 100 μg/mL ampicillin, 10 μg/mL tetracycline, and 0.1% glucose at 27 °C with shaking at 200 rpm. The following day, the cell culture was diluted in 500 mL of LB medium containing the same additives as mentioned above. Cells were grown at 27 °C until an OD_{600} of 0.25 was reached. The culture was induced with 1 mM isopropyl β-D-1-thiogalactopyranoside (IPTG) and 0.2% (w/v) L(+)-arabinose. Cells were collected after overnight expression at 5000 rpm and 4 °C for 15 min. Cell pellet was stored at −20 °C or directly used for protein purification.

Protein Purification by Affinity Chromatography. Protein was purified by affinity chromatography using a method described by Airenne et al.[45] The cell pellet from 1 L of culture was dissolved in 150 mL of 50 mM sodium carbonate, 1 M NaCl, 2 mM EDTA, pH 11. The cell suspension was homogenized twice using an EmulsiFlex C3 homogenizer (Avestin Inc., Ottawa, Canada) using guiding pressure set to 40 psi to obtain a homogenizing pressure of

dx.doi.org/10.1021/bc500462w | *Bioconjugate Chem.* 2014, 25, 2233−2243

15 000 psi. The crude cell lysate was clarified by centrifugation at 16 000*g* and 4 °C for 60 min. The cleared lysate was mixed with 1.5 mL of 2-iminobiotin Sepharose 4 Fast flow (Affiland S.A., Ans Liege, Belgium) and incubated for 2 h at 4 °C followed by centrifugation at 1000*g* for 15 min. The supernatant was removed and the resin was washed with 200 mL of buffer and centrifuged again. The wash step was repeated, after which the Sepharose was transferred to an Econo-Pac column (BioRad Laboratories Inc., Hercules, CA, USA) and additionally washed with 50 mL of buffer by gravity flow. The protein was eluted from the 2-iminobiotin Sepharose with 50 mM Na-acetate, pH 4.0. The protein concentrations in the eluted fractions were determined using the theoretical molar absorption coefficient of the mutants at 280 nm (23 615 M^{-1} cm^{-1}) and the estimated molecular weight (14 300 g/mol). The A_{280} values were measured using a NanoDrop 2000 (Thermo Scientific, Wilmington, DE, USA). The molecular size and purity of the protein were analyzed by SDS-PAGE (15% gel) and subsequent Coomassie brilliant blue staining. A molecular marker (Page Ruler Prestained Protein Ladder, Fermentas) was used for size determination.

Isoelectric Focusing. Isoelectric points of neutralized mutants were analyzed on Immobiline DryStrips pH 3−11 NL, 13 cm (GE Healthcare/Amersham Biosciences AB, Uppsala, Sweden). Proteins were dialyzed to H_2O. For each mutant, 15 μg of non-neutralized form and 15 μg of neutralized form were diluted in 2% Pharmalyte 3−10 for IEF (GE Healthcare) containing 3.75 mg DeStreak reagent (GE Healthcare) in a volume of 250 μL. DryStrip was rehydrated using sample solution at 20 °C for 6 h. Samples were run in Ettan IPGphor3 IEF unit (GE Healthcare) for 5.3 h at 20 V, for 45 min at 150 V, for 45 min at 300 V, for 45 min at 600 V, and then with a linear gradient from 600 to 5000 V in 1 h, followed by a linear gradient from 5000 to 8000 V in 1 h. Finally, the run was continued at 8000 V for 6.1 h. After focusing, the DryStrips were fixed in 20% TCA for 10 min, followed by a wash with destaining solution (0.1% $CuSO_4$, 10% acetic acid, 30% methanol) for 2 min. The DryStrips were stained with staining solution (0.25% Coomassie blue, 30% methanol, 0.1% $CuSO_4$, 10% acetic acid) for 1 h. DryStrips were destained in destaining solution for overnight. DryStrips were impregnated in 5% glycerol, 10% acetic acid for 10 min and air-dried. The isoelectric point was determined by comparison with standard protein IEF mix 3.6−9.3 (Sigma-Aldrich, St. Louis, MO, USA).

Size-Exclusion Chromatography (SEC). The molecular size of the proteins in solution was measured by size-exclusion chromatography using a Superdex200 10/300GL column connected to an ÄKTA purifier-100 equipped with a UV-900 monitor (GE Healthcare/Amersham Biosciences AB, Uppsala, Sweden). As the mobile phase, PBS, pH 7.3, was used. Approximately 50 μg of protein was injected per run. D-Biotin was added to the samples in 4-fold higher molar concentration. All analyses were performed at a flow rate of 0.5 mL/min and were executed at RT. Absorbance at 280 nm was used to detect the protein peaks in the chromatograms. A molecular weight calibration curve was prepared by using a gel filtration standard protein mixture containing thyroglobulin (670 kDa), γ-globulin (158 kDa), ovalbumin (44 kDa), and myoglobin (17 kDa) (Bio-Rad).

Differential Scanning Calorimetry (DSC). The thermal stability of the studied proteins in the presence and absence of ligand was analyzed using an automated VP-Capillary DSC System (Microcal Inc., Northampton, MA, USA). Thermograms were recorded between 20 and 140 °C with a heating rate of 120 °C/h. Proteins were dialyzed into 50 mM NaH_2PO_4/Na_2HPO_4, 100 mM, pH 7. Samples were degassed prior to measurement. The protein concentration in the cell was 30 μM, and the biotin concentration was 105 μM. Results were analyzed using the Origin 7.0 DSC software suite (Microcal Inc.). Examples of DSC thermograms corresponding to the data shown in Table 1 are shown in Figure S4.

Fluorescence Spectroscopy. The dissociation rate constant (k_{diss}) of fluorescently labeled biotin was determined by fluorescence spectrometry using the biotin-labeled fluorescent probe ArcDia BF560 (ArcDia, Turku, Finland BF560) as described in Hytönen et al.[43] or biotin−4-fluorescein (Sigma-Aldrich). In principle, the changes in the fluorescence intensity of a 50 nM dye in 50 mM NaH_2PO_4/Na_2HPO_4, 650 mM NaCl, 0.1 mg/mL BSA, pH 7, were measured after the addition of 100 nM biotin-binding protein. The dissociation of this complex was observed by addition of a 100-fold molar excess of free biotin. The assay was performed at 50 °C using a QuantaMaster Spectrofluorometer (Photon Technology International, Inc., Lawrenceville, NJ, USA). The biotinylated BF560 was excited at 560 nm, and emission was measured at 578 nm. Biotin−4-fluorescein was excited at 494 nm, and emission was measured at 521 nm.

The association rate constant (k_{ass}) of fluorescent probe ArcDia BF560 to the analyzed mutants was determined in a similar experimental setup as that used for the dissociation rate. Protein (2.5, 5, or 10 nM) was added to 50 nM dye in 50 mM NaH_2PO_4/Na_2HPO_4, 650 mM NaCl, 0.1 mg/mL BSA, pH 7, stirred continuously with a magnetic stirrer. The association of fluorescence probe to protein was measured for 300 s. To analyze the data, a simple equation of exponential decay was fitted to the measured data using an unweighted least-squares method. Because the protein sample was injected into the cuvette through an opening in the lid of the spectrofluorometer, the ongoing measurement was perturbed as the tip of the pipet entered the path of the light beam and bubbles were formed at the end of the injection. Moreover, the mixing of the two solutions took time. These perturbations were momentary, but the data affected by it needed to be identified and excluded from the data analysis. This was done by calculating the *k*-value with different starting times and comparing the results. In an ideal case, all *k*-values would be the same. In reality, the fitting tends to yield a consistent value for *k* from only 1 or 2 s after the injection. The reported k_{ass} values are averages of the consistent values.

Radioactive [^{3}H]Biotin Assay. The dissociation rate constant (k_{diss}) of *d*-[8,9-^{3}H(*N*)]-biotin (PerkinElmer, Boston, MA, USA) was determined at 50 °C by competition with free biotin as described in Klumb et al.[46] Measurements were carried out in a 50 mM NaH_2PO_4/Na_2HPO_4 buffer (pH 7) containing 100 mM NaCl and 10 μg/mL BSA to prevent nonspecific binding. Counts of radioactive biotin (10 nM) were measured before the addition of proteins to a concentration of 50 nM. The level of unbound radioactive biotin was subsequently measured. An excess of normal biotin was added to the samples to replace bound radioactive biotin. The amount of free radioactive biotin was used to determine k_{diss} from the slope of the best-fit line in a plot of ln(fraction of bound biotin) versus time, as described earlier by Klumb et al.[46] Free *d*-[8,9-^{3}H(*N*)]-biotin was assayed for radioactivity in a liquid scintillation counter (Tri-Carb 2910 TR, PerkinElmer, Walthman, MA, USA).

dx.doi.org/10.1021/bc500462w | *Bioconjugate Chem.* 2014, 25, 2233−2243

Surface Plasmon Resonance Biosensing. All experiments were performed on a Biacore X instrument, as previously described for avidin M96H.[20] Specific binding (hybridization) and nonspecific adsorption of DNA on monolayers of switchavidin, avidin M96H, and avidin M96H/R114L was determined on self-assembled monolayers with 20% biotin content. The chip was treated with BSA and SDS, after which a monolayer of avidin mutant was formed in flow cell 2 (FC2, blue trace). The monolayer in FC2 was selectively functionalized with the biotinylated DNA (5′-biotin-GCACCTGACTCCTGTGGAGAAGTCTGCCGT),[47] and both flow cells were washed with buffer injections to remove biotinylated DNA from the microfluidic system. Subsequently, avidin mutant protein was injected in FC1 (red trace), followed by injection of BSA in both flow cells. Then, the identical DNA strand but without a biotin label (unlabeled probe, 5′-GCACCTGACTCCTGTGGAGAAGTCTGCCGT) was injected in both flow cells in order to monitor the nonspecific adsorption in both flow cells. Finally, the complementary DNA strand (analyte, digoxigenin-5′-ACGGCAGACTTCTCCACAGGAGTCAGGTGC) was injected in both flow cells, giving rise to nonspecific binding in FC1 and to specific plus nonspecific binding in FC2, which contained the biotinylated DNA.

Cell Labeling. Fibroblast 3T3 cells in high-glucose (with Na-pyruvate) DMEM, supplemented with 5% FBS, 1% P/S, and 1% L-glutamine, were cultured in 75 cm^2 cell culture flask. The cells were washed twice with warm PBS and treated with a solution containing 200 μg/mL NHS-biotin (EZ-Link NHS-LC-LC-Biotin, Thermo Scientific no. 21343) for 10 min at room temperature. Cells were then washed twice with PBS, followed by trypsination and plating to a fibronectin (fn)-coated glass coverslips. The fn coating of the coverslips was conducted prior to the experiments by incubating the coverslip in a 50 μg/mL solution of human plasma fn in PBS for 1 h, followed by 3× wash with PBS. Biotinylated cells were allowed to adhere to the fn-coated coverslips for 30 min and were then washed with PBS and fixed with 4% PFA in PBS. The cells were labeled with a 1:100 dilution of Alexa Fluor 555-conjugated phalloidin (Life Technologies, no. A34055) together with 10 μg/mL Alexa Fluor 488-labeled switchavidin or Alexa Fluor 488-labeled WT avidin produced in *E. coli* for 30 min at RT. Negative controls were prepared by first incubating the avidins in a solution containing 10 μg/mL free biotin. Finally, the samples were washed twice with PBS and embedded using Prolong Gold antifade agent with DAPI (Life Technologies no. P-36931).

Fluorescence microscopy of the cells was performed by using Zeiss LSM780 confocal system on Zeiss Cell Observer microscope and using Plan-Apochromat 20×/0.8 dry objective (Zeiss, Jena, Germany). DAPI, Alexa Fluor 488, and Alexa Fluor 555 were excited using 405, 488, and 561 nm laser lines, respectively. Fluorescence emission bands were selected to avoid overlap, and scanning was conducted sequentially to negate spectral bleed through.

Regeneration of Biotinylated Glass Coverslips. The 18 × 18 mm^2 coverslips were washed by immersing them in 70% ethanol, followed by immersion in distilled water to remove any contaminants. The coverslips were placed on a hot plate at 80 °C, and 400 μL of 0.1 M NaOH was added to the coverslip so that the solution covered the entire glass surface. The 0.1 M NaOH solution was evaporated completely on the hot plate at 80 °C, leaving a white uniform layer of NaOH. The coverslips were removed from the hot plate, and 100 μL of (3-aminopropyl)triethoxysilane (APTES) (Sigma-Aldrich) was added to the surface of the coverslips and left in the fume hood for 5 min to react, before washing the coverslips thoroughly with distilled water. After allowing the coverslips to dry, 200 μL of 0.5% glutaraldehyde solution in H_2O (Sigma-Aldrich) was added to each coverslip and incubated for 30 min. The coverslips were washed with distilled water and left to dry. After glutaraldehyde treatment, the coverslips were mounted on a 3 mL dish containing a hole on it. Biotinylated BSA (approximately 1 biotin/BSA) in 1 mg/mL concentration was applied in 0.5 μL drops on selected areas of the coverslip and allowed to dry. The remaining surface was blocked with 10 mg/mL BSA in PBS at 37 °C for 30 min. The resulting pattern was investigated using a Zeiss LSM780 confocal microscope (Zeiss) with a 63× water immersion objective. Alexa 488 fluorescently labeled switchavidin in PBS + 1 M NaCl was applied on the surface for 5 min, and the intensity of the pattern edge was measured. The sample was subsequently washed with PBS + 1 M NaCl, followed by regeneration with 2.5% citric acid + 0.25% SDS. After careful washing with PBS, the pattern was again labeled with switchavidin, washed, and regenerated again. This cycle was performed five times in total.

Miscellaneous Methods. The theoretical pI of switchavidin was determined using the ProtParam tool available on the ExPASy webpage (http://web.expasy.org/protparam/). Residues M96 and R114 and mutation R114L were visualized using a crystallographic structure of WT avidin in complex with biotin (PDB ID: 1AVD[48]) and the PyMOL Molecular Graphics System, version 1.5.0.4 (Schrödinger, LLC).

■ ASSOCIATED CONTENT

Supporting Information

Primer sequences used to construct avidin mutants. Table S1: Dissociation of biotin probes from avidin mutants. Table S2: Nonspecific binding of proteins to monolayer of the avidin mutants. Figure S1: Association rate of biotinylated fluorescent probe ArcDia BF560 to analyzed proteins. Figure S2: Size-exclusion chromatography elution diagrams of analyzed proteins in the presence and absence of biotin. Figure S3: Isoelectric focusing gel of switchavidin. Figure S4: Thermograms from differential scanning calorimetry analysis. This material is available free of charge via the Internet at http://pubs.acs.org.

■ AUTHOR INFORMATION

Corresponding Author

*E-mail: vesa.hytonen@uta.fi.

Notes

The authors declare no competing financial interest.

■ ACKNOWLEDGMENTS

Technical assistance by Ulla Kiiskinen, Laura Kananen, Juho Rinne, Daniel Eichinger, Clemens Flattinger, and Bianca Spitzbart is gratefully acknowledged. Eric Dufour and Giuseppe Cannino are acknowledged for their help with isoelectric focusing. This research was funded by grants 136288 and 273192 from the Academy of Finland (to V.P.H.), by the National Doctoral Program in Informational and Structural Biology (ISB), and by the Austrian Research Promotion Agency (FFG, Austrian Nanoscience Initiative VO104-08-BI, project 819703 NSI-NABIOS, to H.J.G.). The NMR

spectrometers used for characterization of the self-assembled monolayer components were acquired in collaboration with the University of South Bohemia (CZ) with financial support from the European Union through the EFRE INTERREG IV ETC-AT-CZ program (project M00146, "RERI-uasb"). We acknowledge infrastructure support from Biocenter Finland.

REFERENCES

(1) Green, N. M. (1990) Avidin and streptavidin. *Methods Enzymol. 184*, 51−67.
(2) Barker, D. F., and Campbell, A. M. (1981) The birA gene of *Escherichia coli* encodes a biotin holoenzyme synthetase. *J. Mol. Biol. 146*, 451−467.
(3) Bayer, E. A., and Wilchek, M. (1990) Application of avidin−biotin technology to affinity-based separations. *J. Chromatogr. 510*, 3−11.
(4) de Boer, E., Rodriguez, P., Bonte, E., Krijgsveld, J., Katsantoni, E., Heck, A., Grosveld, F., and Strouboulis, J. (2003) Efficient biotinylation and single-step purification of tagged transcription factors in mammalian cells and transgenic mice. *Proc. Natl. Acad. Sci. U.S.A. 100*, 7480−7485.
(5) Tykvart, J., Sacha, P., Barinka, C., Knedlik, T., Starkova, J., Lubkowski, J., and Konvalinka, J. (2012) Efficient and versatile one-step affinity purification of *in vivo* biotinylated proteins: expression, characterization and structure analysis of recombinant human glutamate carboxypeptidase II. *Protein Expression Purif. 82*, 106−115.
(6) Korpanty, G., Grayburn, P. A., Shohet, R. V., and Brekken, R. A. (2005) Targeting vascular endothelium with avidin microbubbles. *Ultrasound Med. Biol. 31*, 1279−1283.
(7) Aswathy, J., Jahnavi, S., Krishna, R., Manzoor, K., Nair, S., and Menon, D. (2011) Targeted labeling of cancer cells using biotin tagged avidin functionalized biocompatible fluorescent nanocrystals. *J. Nanosci. Nanotechnol. 11*, 7611−7620.
(8) Jung, K. H., Park, J. W., Paik, J. Y., Quach, C. H., Choe, Y. S., and Lee, K. H. (2012) EGF receptor targeted tumor imaging with biotin-PEG-EGF linked to ^{99m}Tc-HYNIC labeled avidin and streptavidin. *Nucl. Med. Biol. 39*, 1122−1127.
(9) Morgan, H., and Taylor, D. M. (1992) A surface plasmon resonance immunosensor based on the streptavidin-biotin complex. *Biosens. Bioelectron. 7*, 405−410.
(10) Nguyen, B., Tanious, F. A., and Wilson, W. D. (2007) Biosensor-surface plasmon resonance: quantitative analysis of small molecule-nucleic acid interactions. *Methods 42*, 150−161.
(11) Rybak, J. N., Scheurer, S. B., Neri, D., and Elia, G. (2004) Purification of biotinylated proteins on streptavidin resin: a protocol for quantitative elution. *Proteomics 4*, 2296−2299.
(12) Holmberg, A., Blomstergren, A., Nord, O., Lukacs, M., Lundeberg, J., and Uhlen, M. (2005) The biotin−streptavidin interaction can be reversibly broken using water at elevated temperatures. *Electrophoresis 26*, 501−510.
(13) Nguyen, G. H., Milea, J. S., Rai, A., and Smith, C. L. (2005) Mild conditions for releasing mono and bis-biotinylated macromolecules from immobilized streptavidin. *Biomol. Eng. 22*, 147−150.
(14) Wu, S. C., and Wong, S. L. (2005) Engineering soluble monomeric streptavidin with reversible biotin binding capability. *J. Biol. Chem. 280*, 23225−23231.
(15) Morag, E., Bayer, E. A., and Wilchek, M. (1996) Reversibility of biotin-binding by selective modification of tyrosine in avidin. *Biochem. J. 316*, 193−199.
(16) Takakura, Y., Sofuku, K., and Tsunashima, M. (2013) Tamavidin 2-REV: an engineered tamavidin with reversible biotin-binding capability. *J. Biotechnol. 164*, 19−25.
(17) Yuan, Y. J., Gopinath, S. C. B., and Kumar, P. K. R. (2011) Regeneration of commercial biacore chips to analyze biomolecular interactions. *Opt. Eng. 50*, 034402−1−034402−6.
(18) Hodnik, V., and Anderluh, G. (2010) Capture of intact liposomes on biacore sensor chips for protein−membrane interaction studies. *Methods Mol. Biol. 627*, 201−211.
(19) Bergsmann, J., Derler, I., Muik, M., Frischauf, I., Fahrner, M., Pollheimer, P., Schwarzinger, C., Gruber, H. J., Groschner, K., and Romanin, C. (2011) Molecular determinants within N terminus of Orai3 protein that control channel activation and gating. *J. Biol. Chem. 286*, 31565−31575.
(20) Pollheimer, P., Taskinen, B., Scherfler, A., Gusenkov, S., Creus, M., Wiesauer, P., Zauner, D., Schofberger, W., Schwarzinger, C., Ebner, A., Tampe, R., Stutz, H., Hytonen, V. P., and Gruber, H. J. (2013) Reversible biofunctionalization of surfaces with a switchable mutant of avidin. *Bioconjugate Chem. 24*, 1656−1668.
(21) Qiu, C., Kumar, S., Guo, J., Yu, L., Guo, W., Shi, S., Russo, J. J., and Ju, J. (2012) Design and synthesis of cleavable biotinylated dideoxynucleotides for DNA sequencing by matrix-assisted laser desorption/ionization time-of-flight mass spectrometry. *Anal. Biochem. 427*, 193−201.
(22) Nordlund, H. R., Hytönen, V. P., Laitinen, O. H., Uotila, S. T., Niskanen, E. A., Savolainen, J., Porkka, E., and Kulomaa, M. S. (2003) Introduction of histidine residues into avidin subunit interfaces allows pH-dependent regulation of quaternary structure and biotin binding. *FEBS Lett. 555*, 449−454.
(23) Pazy, Y., Kulik, T., Bayer, E. A., Wilchek, M., and Livnah, O. (2002) Ligand exchange between proteins. exchange of biotin and biotin derivatives between avidin and streptavidin. *J. Biol. Chem. 277*, 30892−30900.
(24) Hayouka, R., Eisenberg-Domovich, Y., Hytönen, V. P., Maatta, J. A., Nordlund, H. R., Kulomaa, M. S., Wilchek, M., Bayer, E. A., and Livnah, O. (2008) Critical importance of loop conformation to avidin-enhanced hydrolysis of an active biotin ester. *Acta Crystallogr., Sect. D: Biol. Crystallogr. 64*, 302−308.
(25) Chivers, C. E., Crozat, E., Chu, C., Moy, V. T., Sherratt, D. J., and Howarth, M. (2010) A streptavidin variant with slower biotin dissociation and increased mechanostability. *Nat. Methods 7*, 391−393.
(26) Levy, M., and Ellington, A. D. (2008) Directed evolution of streptavidin variants using in vitro compartmentalization. *Chem. Biol. 15*, 979−989.
(27) Brandts, J. F., and Lin, L. N. (1990) Study of strong to ultratight protein interactions using differential scanning calorimetry. *Biochemistry 29*, 6927−6940.
(28) González, M., Bagatolli, L. A., Echabe, I., Arrondo, J. L., Argarana, C. E., Cantor, C. R., and Fidelio, G. D. (1997) Interaction of biotin with streptavidin. thermostability and conformational changes upon binding. *J. Biol. Chem. 272*, 11288−11294.
(29) Katz, B. A. (1997) Binding of biotin to streptavidin stabilizes intersubunit salt bridges between Asp61 and His87 at low pH. *J. Mol. Biol. 274*, 776−800.
(30) Jones, M. L., and Kurzban, G. P. (1995) Noncooperativity of biotin binding to tetrameric streptavidin. *Biochemistry 34*, 11750−11756.
(31) Livnah, O., Bayer, E. A., Wilchek, M., and Sussman, J. L. (1993) Three-dimensional structures of avidin and the avidin−biotin complex. *Proc. Natl. Acad. Sci. U.S.A. 90*, 5076−5080.
(32) Hytönen, V. P., Määttä, J. A., Nyholm, T. K., Livnah, O., Eisenberg-Domovich, Y., Hyre, D., Nordlund, H. R., Horha, J., Niskanen, E. A., Paldanius, T., Kulomaa, T., Porkka, E. J., Stayton, P. S., Laitinen, O. H., and Kulomaa, M. S. (2005) Design and construction of highly stable, protease-resistant chimeric avidins. *J. Biol. Chem. 280*, 10228−10233.
(33) Hyre, D. E., Amon, L. M., Penzotti, J. E., Le Trong, I., Stenkamp, R. E., Lybrand, T. P., and Stayton, P. S. (2002) Early mechanistic events in biotin dissociation from streptavidin. *Nat. Struct. Biol. 9*, 582−585.
(34) Sano, T., and Cantor, C. R. (1995) Intersubunit contacts made by tryptophan 120 with biotin are essential for both strong biotin binding and biotin-induced tighter subunit association of streptavidin. *Proc. Natl. Acad. Sci. U.S.A. 92*, 3180−3184.
(35) Laitinen, O. H., Airenne, K. J., Marttila, A. T., Kulik, T., Porkka, E., Bayer, E. A., Wilchek, M., and Kulomaa, M. S. (1999) Mutation of a critical tryptophan to lysine in avidin or streptavidin may explain why

sea urchin fibropellin adopts an avidin-like domain. *FEBS Lett. 461*, 52−58.
(36) Qureshi, M. H., Yeung, J. C., Wu, S. C., and Wong, S. L. (2001) Development and characterization of a series of soluble tetrameric and monomeric streptavidin muteins with differential biotin binding affinities. *J. Biol. Chem. 276*, 46422−46428.
(37) Marttila, A. T., Laitinen, O. H., Airenne, K. J., Kulik, T., Bayer, E. A., Wilchek, M., and Kulomaa, M. S. (2000) Recombinant NeutraLite avidin: a non-glycosylated, acidic mutant of chicken avidin that exhibits high affinity for biotin and low non-specific binding properties. *FEBS Lett. 467*, 31−36.
(38) Hytönen, V. P., Määttä, J. A., Kidron, H., Halling, K. K., Hörhä, J., Kulomaa, T., Nyholm, T. K., Johnson, M. S., Salminen, T. A., Kulomaa, M. S., and Airenne, T. T. (2005) Avidin related protein 2 shows unique structural and functional features among the avidin protein family. *BMC Biotechnol. 5*, 28.
(39) Eisenberg-Domovich, Y., Hytönen, V. P., Wilchek, M., Bayer, E. A., Kulomaa, M. S., and Livnah, O. (2005) High-resolution crystal structure of an avidin-related protein: Insight into high-affinity biotin binding and protein stability. *Acta Crystallogr., Sect. D: Biol. Crystallogr. 61*, 528−538.
(40) Gast, A. P., Robertson, C. R., Wang, S. W., and Yatcilla, M. T. (1999) Two-dimensional streptavidin crystals: macropatterns and micro-organization. *Biomol. Eng. 16*, 21−27.
(41) Sternberg, E., Persson, B., Hakan, R., and Urbaniczky, C. (1991) Quantitative determination of surface concentration of protein with surface plasmon resonance using radiolabeled proteins. *J. Colloid Interface Sci. 143*, 513−526.
(42) Lahiri, J., Isaacs, L., Tien, J., and Whitesides, G. M. (1999) A strategy for the generation of surfaces presenting ligands for studies of binding based on an active ester as a common reactive intermediate: a surface plasmon resonance study. *Anal. Chem. 71*, 777−790.
(43) Hytönen, V. P., Laitinen, O. H., Airenne, T. T., Kidron, H., Meltola, N. J., Porkka, E. J., Hörhä, J., Paldanius, T., Määttä, J. A., Nordlund, H. R., Johnson, M. S., Salminen, T. A., Airenne, K. J., Yla-Herttuala, S., and Kulomaa, M. S. (2004) Efficient production of active chicken avidin using a bacterial signal peptide in *Escherichia coli*. *Biochem. J. 384*, 385−390.
(44) Horton, R. M., Hunt, H. D., Ho, S. N., Pullen, J. K., and Pease, L. R. (1989) Engineering hybrid genes without the use of restriction enzymes: gene splicing by overlap extension. *Gene 77*, 61−68.
(45) Airenne, K. J., Oker-Blom, C., Marjomaki, V. S., Bayer, E. A., Wilchek, M., and Kulomaa, M. S. (1997) Production of biologically active recombinant avidin in baculovirus-infected insect cells. *Protein Expression Purif. 9*, 100−108.
(46) Klumb, L. A., Chu, V., and Stayton, P. S. (1998) Energetic roles of hydrogen bonds at the ureido oxygen binding pocket in the streptavidin−biotin complex. *Biochemistry 37*, 7657−7663.
(47) Su, X., Wu, Y. J., Robelek, R., and Knoll, W. (2005) Surface plasmon resonance spectroscopy and quartz crystal microbalance study of streptavidin film structure effects on biotinylated DNA assembly and target DNA hybridization. *Langmuir 21*, 348−353.
(48) Pugliese, L., Coda, A., Malcovati, M., and Bolognesi, M. (1993) Three-dimensional structure of the tetragonal crystal form of egg-white avidin in its functional complex with biotin at 2.7 Å resolution. *J. Mol. Biol. 231*, 698−710.